Journal of Structural Geology, Vol. 11, No. 8, pp. 995 to 1006, 1989
Printed in Great Britain

0191-8141/89 $03.00+0.00

Deformation in the overburden of diapiric evaporite ridges: examples from the Sverdrup Basin, Canadian Arctic Archipelago

J. T. VAN BERKEL*

Department of Geology, University of Toronto, Toronto, Ontario, Canada M5S 1A1

(*Received* 27 *February* 1987; *accepted in revised form* 3 *February* 1989)

Abstract—A structural analysis was made to determine the origin of two large anticlines in clastic sedimentary rocks of the Tertiary Eureka Sound Fold Belt, Canada. Each upright, open anticline is a chain of second-order domes which are cored by evaporite diapirs. The strain pattern in the anticlines was determined by using bedding-parallel slickensides for the sense and direction of shear, and a pressure-solution cleavage in sandstone for the orientation of the *XY*-plane of finite strain. Most slickensides have a major component of dip-slip bedding-parallel shear of normal sense (top side moved down). Near the crests of anticlines, cleavage planes dip at a lower angle and in the same direction as bedding planes, but near the crests of synclines they dip at a steeper angle and in the opposite direction to bedding planes.

The results obtained are incompatible with the strain pattern of folds formed by lateral compression but agree with the strain pattern observed in the overburden of diapiric ridges in laboratory models.

INTRODUCTION

MACROSCOPIC folds in sedimentary sequences of orogenic belts can be formed by: (1) lateral compression; (2) buoyant diapirism; or (3) a combination of (1) and (2). What fold mechanism applies in natural folds may be determined by analyzing the orientation of structural elements, the strain pattern and the geometry of the potentially diapiric (lower density or lower viscosity or both) fold core and the mantling rocks (e.g. Ramberg 1963), and then comparing the results with the results of laboratory models simulating geostatic diapirism. The latter models may be centrifuge (e.g. Ramberg 1967, 1981, Stephansson 1972, Dixon 1974, 1975, Talbot 1977, Schwerdtner *et al.* 1978, Schwerdtner & Tröeng 1978, Dixon & Summers 1983, Morgan 1986), mathematical (Fletcher 1972) or finite element (Mareschal & West 1977, 1980, West & Mareschal 1979).

Anticlinal structures cored by evaporite diapirs in unmetamorposed sedimentary basins are ideal for such a study because the initial state and boundary conditions are known from geological and geophysical studies and from extensive drilling. Two large doubly-plunging anticlines, the North Mokka and Whitsunday Bay anticlines, from a Tertiary fold belt (Eureka Sound Fold Belt, Thorsteinsson & Tozer 1970, Balkwill 1978) in the eastern Sverdrup Basin, Canadian Arctic Archipelago (Fig. 1) will be described in this paper. Both anticlines are pierced by evaporite diapirs (Figs. 1–5). The strain distribution in the anticlines was determined by using bedding-parallel slickensides and pressure-solution cleavage in sandstone (van Berkel *et al.* 1983), and is compared here with the strain pattern of laboratory models of diapiric antiforms.

* Present address: Institute of Earth Sciences, Free University, P.O. Box 7161, 1007 MC Amsterdam, The Netherlands.

GEOLOGICAL SETTING

The North Mokka and Whitsunday Bay anticlines (Figs. 1–5) (Thorsteinsson 1974, map 1302A) are two large, open doubly-plunging anticlines that are characteristic of the central Eureka Sound Fold Belt, Sverdrup Basin, Canadian Arctic Islands (Gould & DeMille 1964). Both anticlines are largely composed of Mesozoic arenites and shale that have been pierced locally by evaporites (Hugon & Schwerdtner 1982, van Berkel *et al.* 1983, 1984, 1986, Schwerdtner & Osadetz 1983, Schwerdtner & van Kranendonk 1984, van Berkel 1986) of the Upper Carboniferous Otto Fiord Formation (Thorsteinsson 1974, Nassichuk & Davis 1980).

The North Mokka and Whitsunday Bay anticlines (Figs. 2 and 4) generally have moderately-dipping limbs (Figs. 6 and 7). The North Mokka anticline is made up of a chain of several small coalescent domes shown schematically in Fig. 8, and the Whitsunday Bay anticline of at least three. Stereoplots of poles to bedding planes from both anticlines are given in Fig. 9. The Mokka Fiord diapir (Schwerdtner & Clark 1967) is located at the south end of the North Mokka anticline. At the present erosion level the evaporite diapirs in the cores of the anticlines are composed of anhydrite with minor limestone interbeds. The Three Lakes diapir (Fig. 3) has a diamond shape in outcrop and its domal axis is tilted to the north or northwest. The diapir is rimmed by a 300–500 m thick unit of anhydrite-bearing marble (about 10% $CaSO_4$). The marble unit is chiefly a recrystallized equivalent of limestone and anhydrite from the Upper Carboniferous Otto Fiord Formation (Thorsteinsson 1974, Nassichuk & Davies 1980). It locally contains up to 30% fragments of limestone, anhydrite and diabase. The conversion of limestone into marble must be closely related to diapirism (van Berkel *et al.* 1983). On the southwest side the internal structure of the Three Lakes

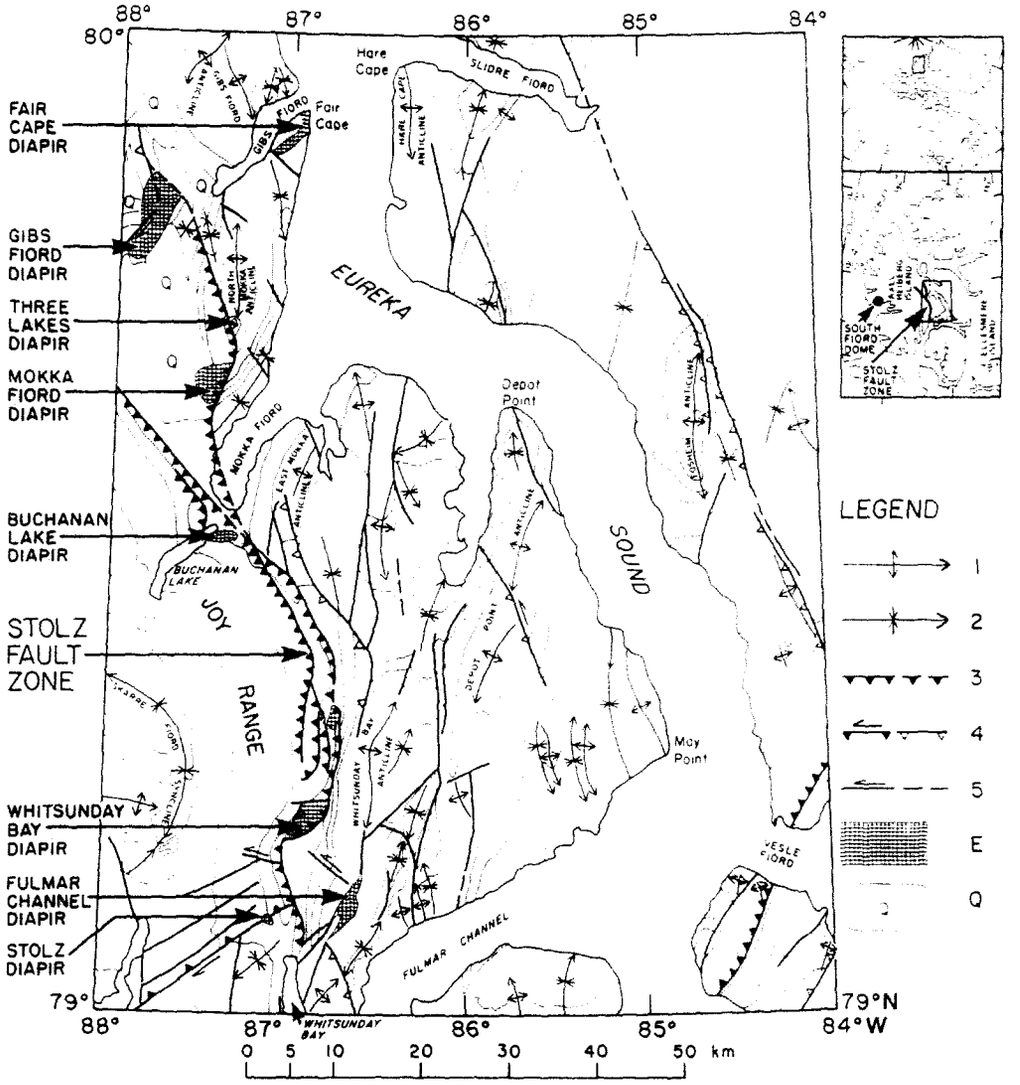

Fig. 1. Tectonic map of eastern Axel Heiberg Island (partly after Thorsteinsson 1974, map 1302A, and van Berkel *et al.* 1983). For simplicity only geologic boundaries are shown. The legend is: 1—anticline with plunge of fold axis; 2—syncline with plunge of fold axis; 3—thrust fault (known, assumed); 4—reverse fault (known, assumed, arrow indicates minor component of horizontal displacement, triangle on up-thrown side); 5—fault (known, inferred); E—evaporite diapir (mainly anhydrite, cored by salt?); Q—Quaternary.

diapir is cut off by a steeply-dipping reverse fault which is a branch of the Stolz fault zone (Fig. 1).

The Fulmar Channel diapir (Fig. 5) has an unusual shape, with a pointed north tail and two pointed south tails. The northwest boundary is straight. A 5–200 m thick, partly cataclastic limestone unit generally marks the boundary. The diapir is built up of two or more subdomes (Fig. 5). Bedding, defined by limestone interbeds, is generally parallel to foliation, defined by deformed anhydrite nodules. On the northwest and southwest sides the internal structure is cut off by steep regional faults.

Regional faults are located in the hinge zones of both anticlines. That in the North Mokka anticline dips steeply to the west. Facing of slickensides steps and flexural drag of strata near the fault indicate that it is a reverse fault. Because younger rocks occur in the hangingwall, the fault plane is probably listric, becoming more shallow to the west (Fig. 6). The dip of the regional faults is steep or vertical in the Whitsunday Bay anticline at the present level of erosion. The orientation of sedimentary strata along the regional fault which follows the northwest margin of the Fulmar Channel diapir suggests that the western block is upthrown with respect to the eastern block. The vertical separation in the Upper Triassic Heiberg Formation is at least 1000 m. There are several small anhydrite bodies found along the regional faults cutting the hinge zones of the North Mokka and Whitsunday Bay anticlines (Figs. 2 and 4).

A major period of mafic intrusive activity during the early Cretaceous (see Jackson & Halls 1985 for a review of available age dates) emplaced diabase sills, and to a lesser extent dykes, in both anticlines. The intrusions, varying in thickness from 1 to 30 m, are especially abundant in the Middle and Upper Triassic Blaa Mountain Formation, where they make up to 25% of a section, but they are never found in the youngest rocks, the Tertiary Eureka Sound Formation. A now highly frac-

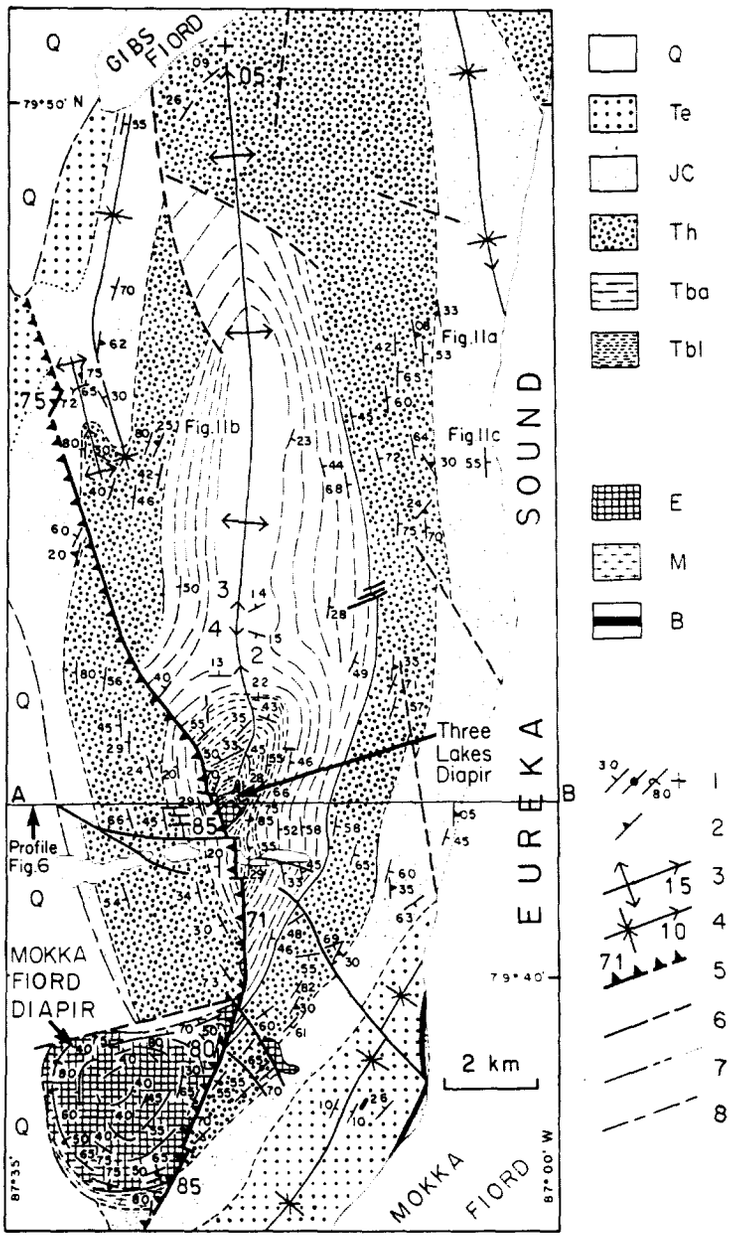

Fig. 2. Geological map of the North Mokka anticline, eastern Axel Heiberg Island (partly after Thorsteinsson 1974, map 1302A, and van Berkel *et al.* 1983). For location see Fig. 1. Topographic relief is between 50 and 500 m. The legend is: Q—Quaternary; Te—Tertiary Eureka Sound Formation (sandstone, siltstone, conglomerate, shale, coal); JC—Cretaceous and Jurassic rocks (sandstone and shale; minor siltstone); Th—Upper Triassic Heiberg Formation (sandstone and siltstone; minor shale); Tba—Lower and Middle Triassic Blaa Mountain Formation (siltstone and shale); Tbl—Lower and Middle Triassic Blind Fiord formation (siltstone; minor shale and rarely limestone); E—evaporite diapir (mainly anhydrite, cored by salt (?), with minor thin limestone interbeds); M—marble, with minor gypsum; B—Upper Cretaceous basalt flow; 1—bedding (inclined, vertical, overturned, horizontal); 2—cleavage in sandstone; 3—anticline with plunge of fold axis; 4—syncline with plunge of fold axis; 5—thrust fault (defined, inferred); 6—fault (defined, inferred); 7—geologic boundary (defined, approximate, concealed); 8—boundary of Quaternary sediments. Form lines are shown in units Tba and Tbl and they are generally parallel to trend lines of bedding, except where the topographic relief is strong, e.g. in the east–west valley south of the Three Lakes diapir.

tured diabase dyke cuts the Three Lakes diapir (Fig. 3). In the Whitsunday Bay anticline the diabase sills northwest of the Fulmar Channel diapir (Fig. 5) stop abruptly at the northwest fault contact of the diapir.

SLICKENSIDES

The sense of bedding-parallel shear can be determined from the facing direction of tiny slickenside fracture steps (e.g. Tjia 1964, 1967, Norris & Barron 1969, Hancock & Barka 1987, Petit 1987) and accretion steps (Norris & Barron 1969). The fracture steps used for determining the sense of shear are the result of small irregularities in the fault plane and are different from risers formed by offsets due to tiny low- or high-angle faults that cross the slickenside planes (Petit 1987). The latter are more likely to form in fault planes with significant displacement whereas the former fracture steps only have small displacements. The lineation of

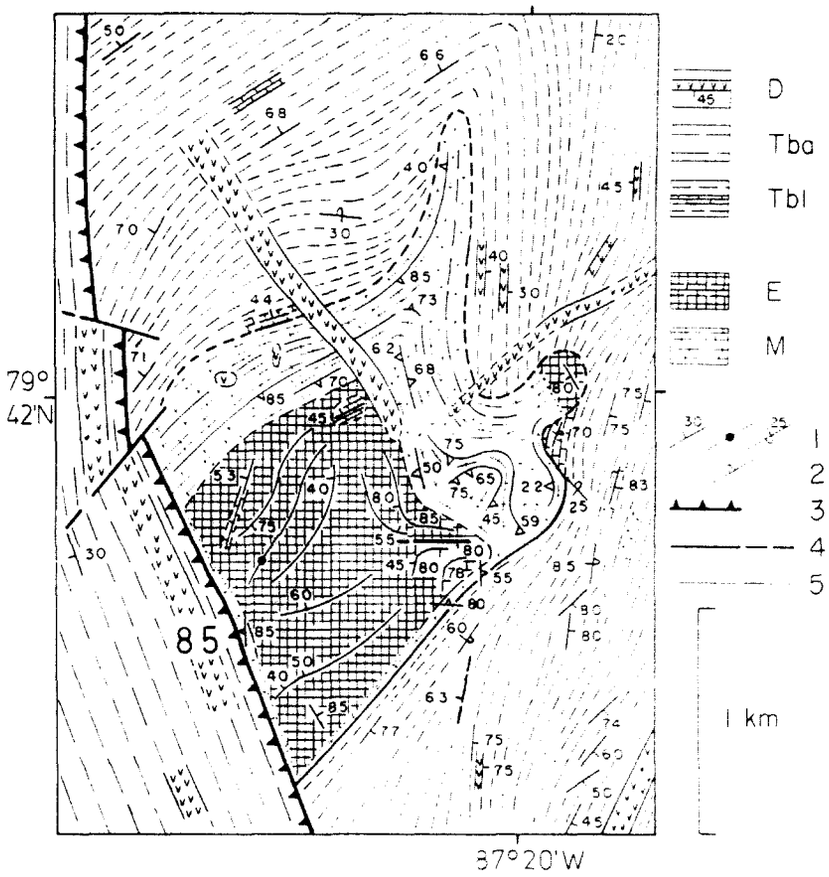

Fig. 3. Geological map of the Three Lakes diapir, located near the centre of the North Mokka anticline. For location see Fig. 2. The legend is as in Fig. 2 with, in addition: D—Upper Cretaceous diabase sills and dykes (with dip of contact); 2—foliation in marble; 3—thrust fault (defined); 4—fault (defined, inferred); 5—geologic boundary (defined, approximate, concealed).

slickensides and the tiny fracture steps which are cut into solid rock can easily be overprinted by younger generation structures. This is clearly visible when the younger slickensides have a different orientation, but when they are parallel to an older generation they are impossible to detect. However, if in a single outcrop most fracture steps of slickensides do have a unique facing orientation, it may be possible to use them to infer sense of movement with a high degree of certainty.

In each outcrop several slickensides with fracture steps on faces parallel to bedding were inspected for consistency and possible overprinting. Faces at an angle to bedding were also studied. In Fig. 10 one representative slickenside, parallel or subparallel to bedding, was plotted per exposure using the method of Hoeppener (1955). In this method the centre of the arrow on the plot corresponds to the pole to the slickenside plane and the arrow shows the trend of the slickenside lineation. In this way the orientation of a slickenside surface and the trend of the lineation on it can be represented with a single arrow. The arrows representing slickensides with a major normal displacement (hangingwall block moved down) component point approximately toward the centre of the stereonet and those with a major reverse displacement (hangingwall block moved up) component point away from the centre. Down-dip slickensides point either exactly toward or away from the centre of the stereonet. In the North Mokka anticline, most slickensides in clastic sediments and diabase reveal that the major component of bedding-parallel shear was dip-slip and normal. Most slickensides with a reverse dip-slip component or only a strike-slip motion occur in the hangingwall of the thrust fault close to the fault plane (label 2 in Fig. 10a; labels 3, 4, 5 and 6 in Fig. 10b) or at the crest of the anticline (labels 1, 4 and 5 in Fig. 10a). Only a few slickensides have a reverse dip-slip component (label 3 in Fig. 10a; labels 1 and 2 in Fig. 9b).

Unfortunately, only seven slickensides were observed in the Whitsunday Bay anticline (Fig. 10c), in which the major component of bedding-parallel shear was also dip-slip and normal. On the other hand, many cleavage readings were taken in sandstone beds of this anticline.

CLEAVAGE IN SANDSTONE

A closely-spaced cleavage in sandstone (van Berkel *et al.* 1983, van Berkel 1985) is observed in well-exposed sections of loosely consolidated Triassic and Jurassic sandstone (Fig. 11). The cleavage is usually planar (Figs. 11b & d), although in some exposures it is slightly sigmoidal on a scale of 20–200 cm (Figs. 11a & c). The cleavage occurs throughout long (50–500 m) well-exposed sections in which it usually is constant in orien-

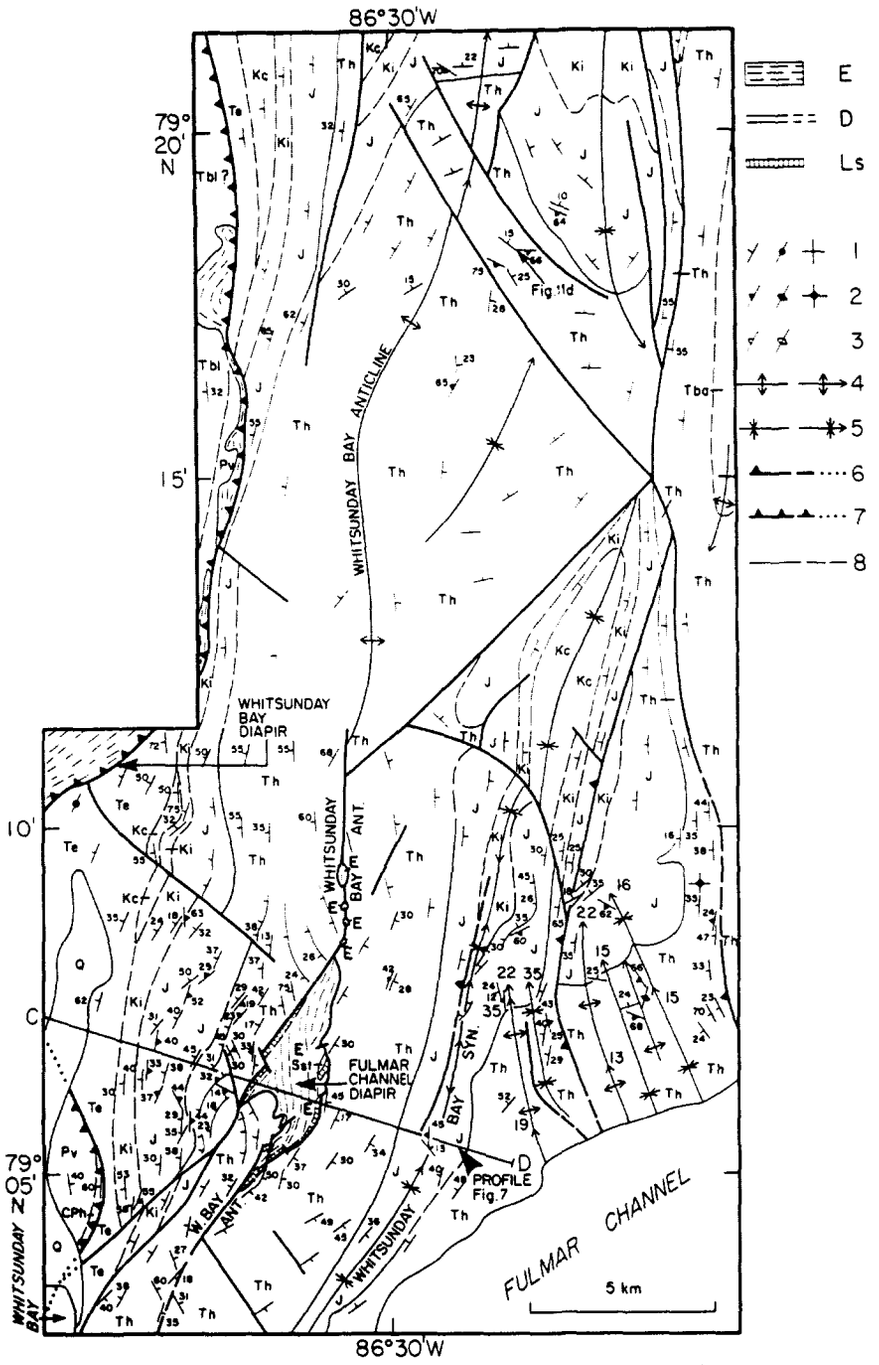

Fig. 4. Geological map of the Whitsunday Bay anticline and the area to the east, eastern Axel Heiberg Island (partly after Thorsteinsson 1974, Map 1302A). For location see Fig. 1. Elevation varies from 0 to 500 m above sea level. See Figs. 2 and 3 for the meaning, but note differences in ornamentation. In addition, note that: Kc—Cretaceous Christopher Formation (mainly shale); Ki—Cretaceous Isachsen Formation (mainly sandstone); J—Jurassic rocks (sandstone and shale; minor siltstone); Pv—Lower Permian Van Hauen Formation (shale and siltstone); CPh—Upper Carboniferous and Lower Permian Hare Fiord Formation (shale and siltstone; minor limestone); Sst—sandstone of unknown age. Also note that: trend lines and minor thin limestone interbeds (Ls) are indicated in the diapir; 1—bedding (inclined, vertical, horizontal); 2—cleavage in sandstone (inclined, vertical, horizontal); 3—foliation defined by deformed anhydrite nodules; 4—anticline with plunge of fold axis; 5—syncline with plunge of fold axis; 6—fault (defined, inferred, concealed; triangles indicate upthrown sides); 7—thrust fault (defined, inferred, concealed); 8—geologic boundary (defined, inferred).

tation. The term cleavage (Borradaile *et al.* 1982) is justified because the rock splits preferentially along closely spaced surfaces, similar to slaty cleavage. Note that frost weathering gives a false impression of the spacing of cleavage planes (Fig. 11), because actual cleavage spacing is much closer than is visible in outcrop. The sandstone cleavage is only seen in loosely consolidated sandstone that would easily weather in a humid climate. The dry, cold polar climate in the Canadian High Arctic seems to be ideal for preserving exposures.

Orientations of cleavage in sandstone were measured in different exposures in the North Mokka and Whitsunday Bay anticlines (Fig. 13). The pattern (Figs. 6 and 7) is very different from what is observed in flexural slip or

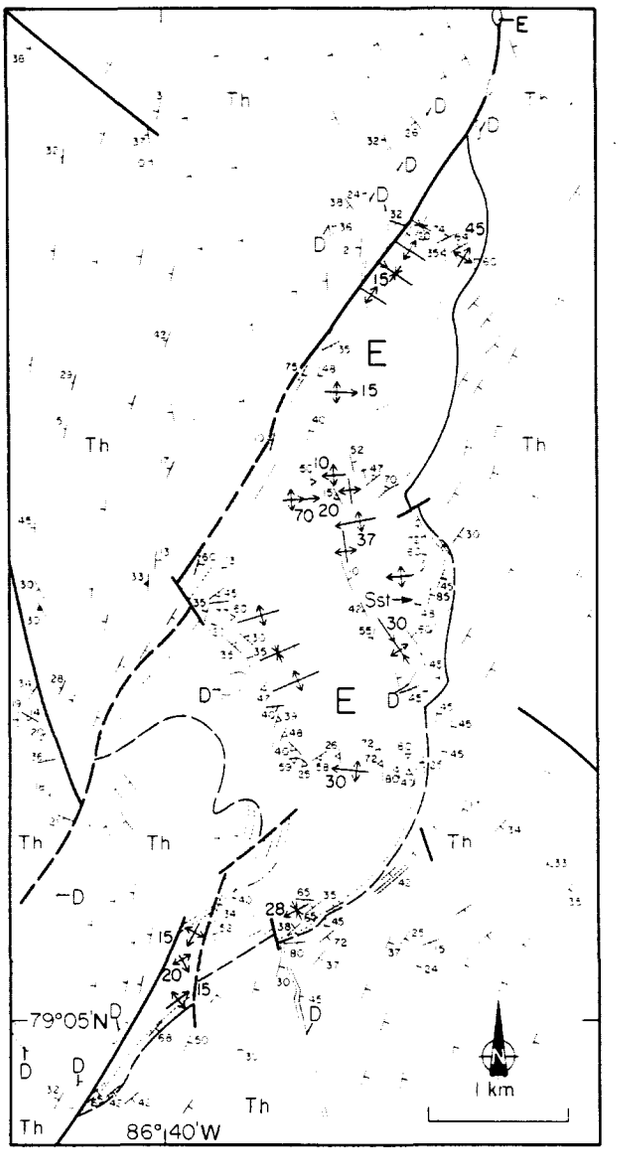

Fig. 5. Geological map of the Fulmar Channel diapir, located near the centre of the Whitsunday Bay anticline. For location and symbols see Figs. 2 and 4.

flexural flow folds formed by lateral compression (e.g. Fig. 14b). In gently-dipping or horizontal strata at the crests of the anticlines, the cleavage is parallel or at a low angle to the bedding (Fig. 14a). In moderate- to steeply-dipping limbs, it dips gently or moderately, in the same direction as the bedding (Figs. 11a–c). In synclines adjacent to the North Mokka and Whitsunday Bay

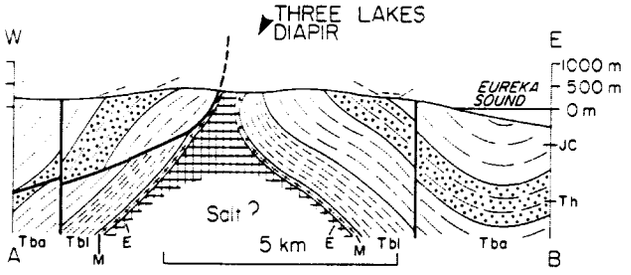

Fig. 6. East–west profile across the North Mokka anticline (Fig. 2) at the Three Lakes diapir (Fig. 3). Dip of sandstone cleavage is indicated by two-dash symbol. For other symbols see Fig. 2.

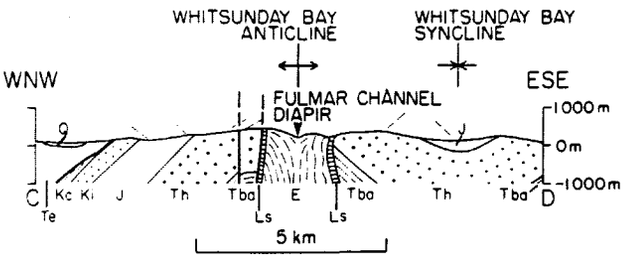

Fig. 7. ESE—WNW profile across the Whitsunday Bay anticline (Fig. 4) at the Fulmar Channel diapir (Fig. 5). Dip of sandstone cleavage is indicated by two-dash symbol. For other symbols see Fig. 4.

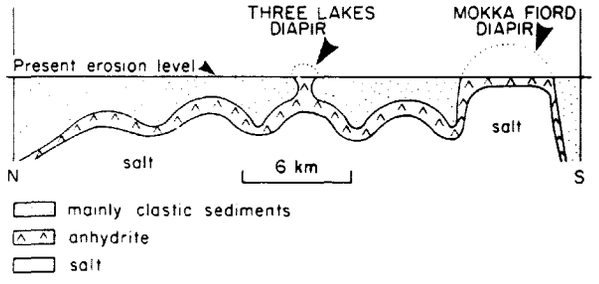

Fig. 8. Idealized N–S profile along the hinge of the North Mokka anticline.

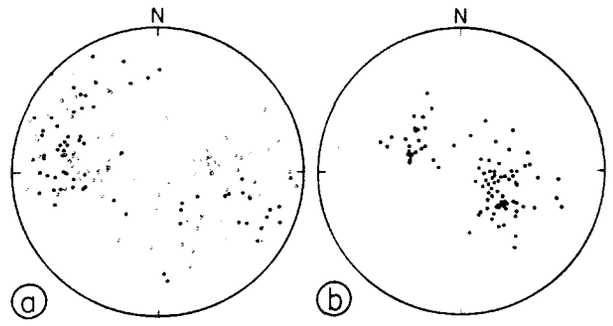

Fig. 9. (a) Equal-area projection (Lambert stereonet) of poles to bedding planes (total 161) in the North Mokka anticline. Filled circles are readings from the area around and south of the Three Lakes diapir. Open circles are readings from the area north of the Three Lakes diapir. (b) Same for the Whitsunday anticline. Readings (total 95) from the area around and south of the Fulmar Channel diapir.

anticlines, the cleavage dips moderately to steeply (in a direction opposite to bedding) or steeply to vertically (Fig. 11d) forming a pattern similar to that of conventional cleavage in compressional flexural-slip or flexural-flow folds (Fig. 14b). Moderately- to steeply-dipping cleavage occurs in some of the smaller anticlines near the North Mokka and Whitsunday Bay anticlines. The steep E–W-striking cleavage in the plunging north end of the Whitsunday Bay anticline (Fig. 4) is an exception to the general cleavage pattern in the anticlines. The microstructure of 20 sandstone specimens was studied. The specimens were taken from the North Mokka and Whitsunday Bay anticlines and the area east of the Whitsunday Bay anticline. Traces of cleavage and bedding as visible in hand specimen were marked on the

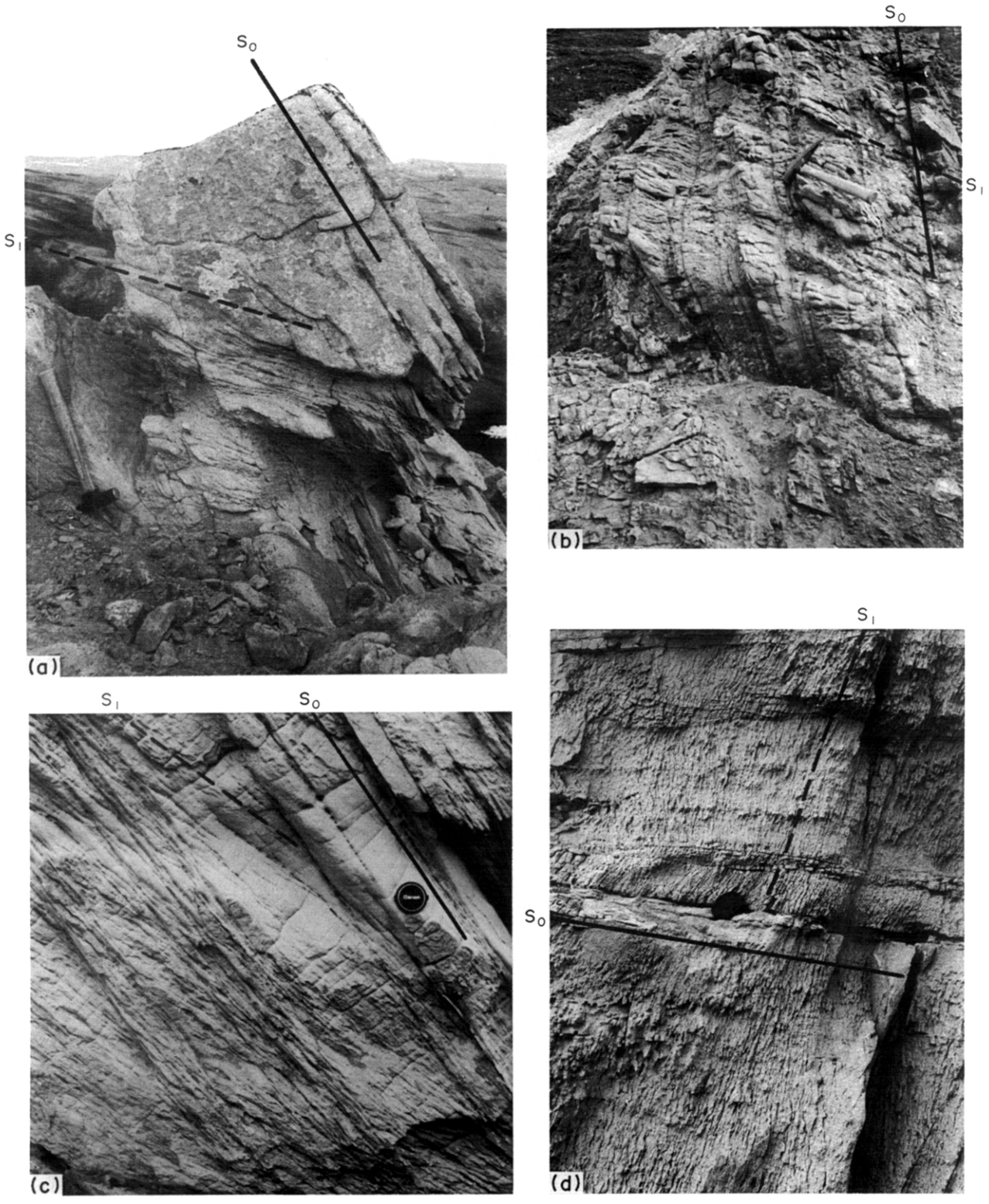

Fig. 11. Cleavage in loosely consolidated sandstone of the Upper Triassic Heiberg Formaton. Bedding is indicated with a solid line and cleavage with a dashed line. For locations see Figs. 2 and 4. (a) Gently-dipping cleavage in moderately-dipping sandstone strata, east limb of the North Mokka anticline. View toward the north. (b) Moderately-dipping, slightly sigmoidal cleavage in steeper-dipping strata, east limb of the North Mokka anticline. View toward the south. (c) Gently-dipping slightly sigmoidal cleavage in steeply inclined strata, west limb of the North Mokka anticline. View toward the north. (d) Steeply-dipping cleavage and gently dipping bedding in sandstone, northeast-side of the Whitsunday Bay anticline. View toward the northwest.

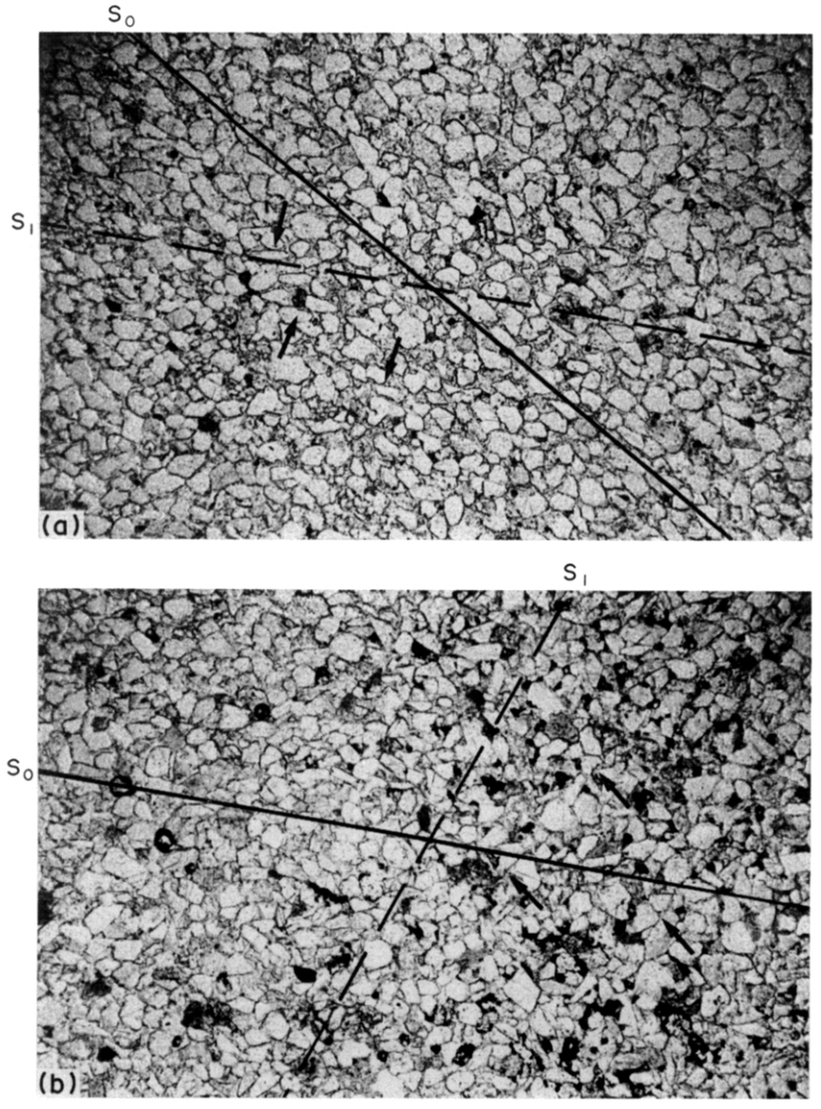

Fig. 12. Photomicrographs (polarized light) of 4 × 2.7 mm areas of samples VB301 (a) and VB313 (b). Sections are normal to bedding and cleavage. The traces of bedding (S_0) and cleavage (S_1) are indicated. Note thin, discontinuous cleavage seams parallel to bedding and cleavage (indicated with arrows). Sample (a) from the exposure shown in Fig. 11(a) and sample (b) from the exposure shown in Fig. 11(d)

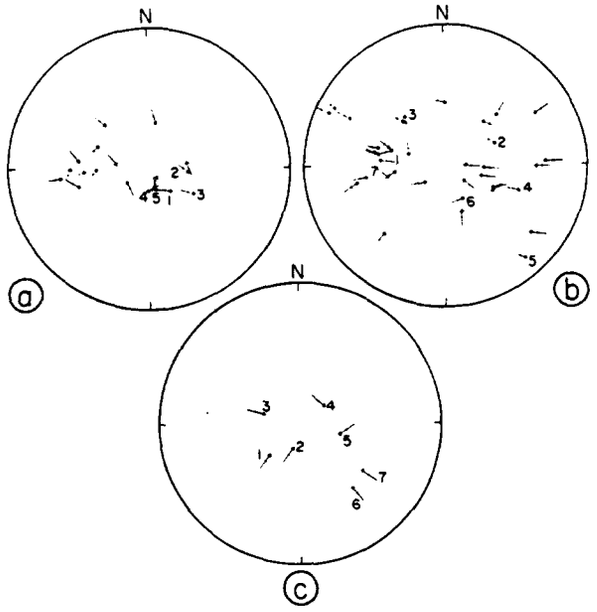

Fig. 10. (a) Stereographic projection (Wulff stereonet) of polished slickensides with fracture steps measured on bedding surfaces in siliciclastic sediments, plotted after the method of Hoeppener (1955). Readings are from the North Mokka anticline. For explanation of labels see text. (b) Like (a), but for slickensides on fractures in diabase subparallel to bedding in siliciclastic sediments. Readings are from the North Mokka anticline. (c) Like (a), but for readings from the Whitsunday Bay anticline. Arrows 1 and 2 are for fractures in sandstone, arrows 3–5 are for fractures in diabase, and arrows 6 and 7 are for bedding surfaces of sandstone.

thin sections and photographs (e.g. Fig. 12) taken of the thin sections.

Grain shape and grain contact orientations

The data presented in this paper are from two localities only. Hand specimen VB301 is from an exposure in the northeast portion of the North Mokka anticline where there is a moderately-dipping bedding and gently-dipping cleavage (Fig. 11a), and VB313 is from the exposure in the northeast portion of the Whitsunday Bay anticline where there is a gently-dipping bedding and steeply-dipping cleavage (Fig. 11d). Results for other samples are consistent with those described here.

In sections perpendicular to bedding and cleavage two kinds of measurement were made: (1) the orientation of

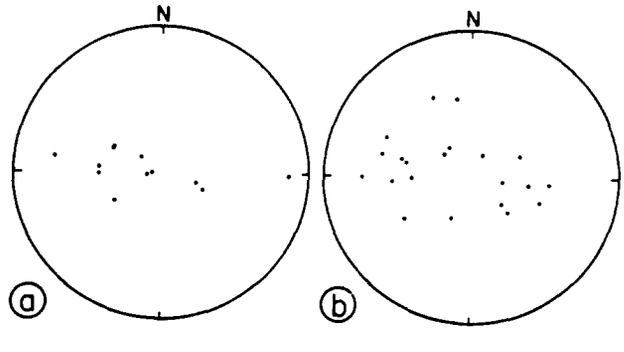

Fig. 13. (a) Equal-area projection (Lambert stereonet) of poles to cleavage in sandstone (total 12) of the North Mokka anticline. (b) Same for the Whitsunday Bay anticline (total 21 readings).

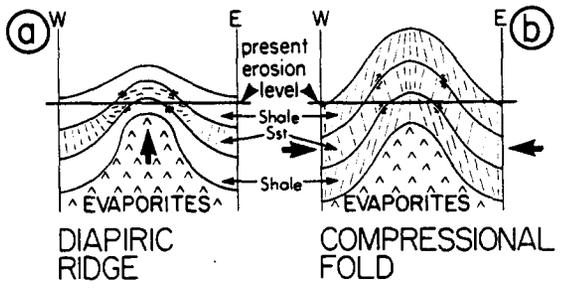

Fig. 14. Schematic cleavage orientation pattern and sense of bedding-parallel shear in antiformal structures. (a) In the North Mokka and Whitsunday Bay anticlines. (b) In an antiform formed by lateral compression. After Ramsay (1967, fig. 7-68).

grain long axes (Fig. 15); and (2) the orientation (number and the sum of length (weighted)) of straight, dented and sutured grain contacts (Fig. 16). Most of the measured grain contacts are likely to have developed by pressure solution. Separate measurements of two different areas of the same thin section were made to check on consistency of results. In histograms for VB301 (Figs. 15a & b and 16a & b), maxima occur between traces of bedding and cleavage. For two different areas of the same thin section the distribution of data in the histograms is similar. However, in histograms for VB313 (Figs. 15c & d and 16c & d) there is no maximum subparallel to the bedding or cleavage trace. In the weighted grain boundary orientation histograms (Figs. 16c & d) a broad maximum occurs in the acute angle between bedding and cleavage.

None of the histograms show evidence for imbrication formed during sedimentation (see Pettijohn *et al.* 1973, p. 369; Potter & Pettijohn 1977, p. 33). In both samples sand grains were originally deposited by laminar flow as can be seen from sedimentary structures. If there was

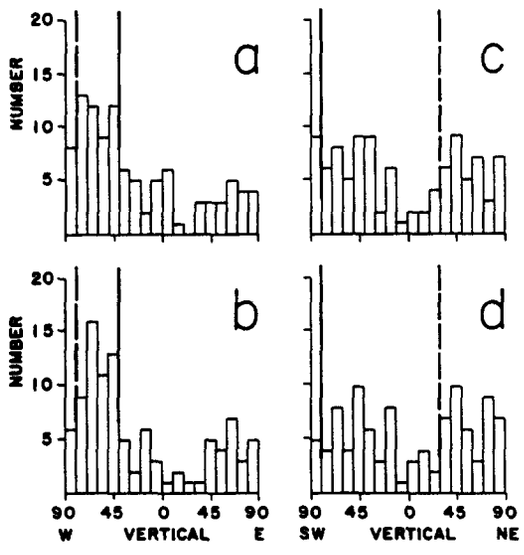

Fig. 15. Distributions of apparent long axis-orientations of quartz grains in sandstone per 10° azimuth interval. Total number of long axes per histogram is 100. The trace of the bedding is indicated by a solid line and the trace of the cleavage by a dashed line. The diagrams are constructed such that the vertical ('0' line) is the true vertical in the exposure (Fig. 11). (a) & (b) For two different 4 × 2.7 mm areas of thin section VB301 (a corresponds to Fig. 12a). (c) & (d). Same for thin section VB313 (c corresponds to Fig. 12c).

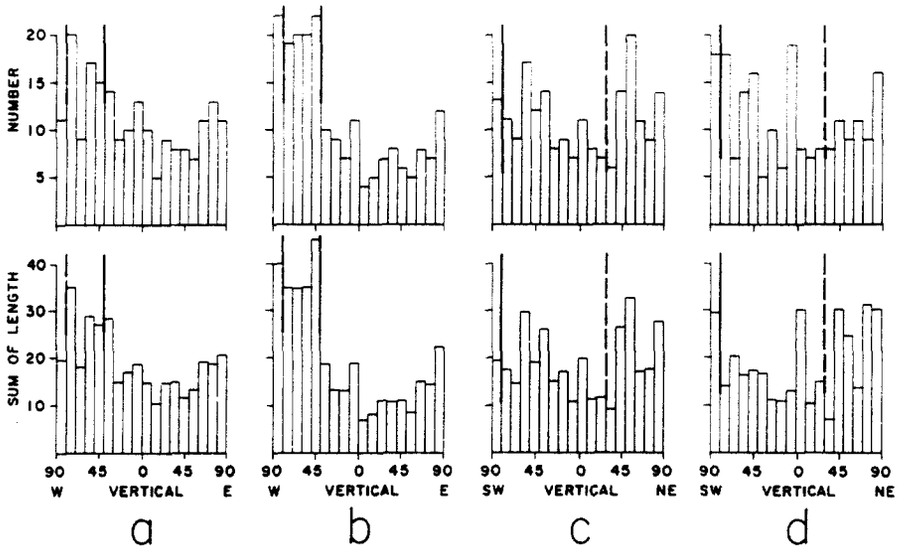

Fig. 16. Distributions of the numbers and sums of lengths (10 units is 0.051 mm) of 200 straight, dented and sutured grain boundaries which show evidence for pressure solution. (a) & (b) Sample VB301. (c) & (d) Sample VB313. Other details as in Fig. 15.

imbrication, it would have caused a skewed or symmetric maximum in the histograms up to 18° clockwise from the bedding, because the currents that deposited the sediments in the study area were toward the west, northwest or west-northwest (Embry 1982).

An examination was made of two sandstone hand specimens from exposures with joints but without a cleavage. In these exposures the bedding dips gently and the joints are vertical with a spacing of 1–5 cm. A weak maximum coincides with the trace of bedding and the distribution around the maximum is broad and symmetric, but there is no maximum parallel to the trace of the joints.

Interpretation of results

Pressure solution is a cleavage-forming process during deformation of low-grade metamorphic sandstones, arenites and wackes (Plessman 1963, Williams 1972, Gray 1978, Borradaile *et al.* 1982). Dissolution of quartz and feldspar leads to seams enriched in mica and to preferential dimensionally-oriented quartz and feldspar grains. Cleavage spacing depends on the density of mica seams. Pressure solution may be an active process at very low *P–T* conditions during deformation (e.g. Durney 1972).

Pressure solution perpendicular to bedding is also common during burial of loosely consolidated porous sandstone (e.g. Heald 1956, Sibley & Blatt 1976). It may create dented, concavo-convex or sutured grain boundaries. Micas between quartz grains encourage dissolution (e.g. Heald 1956). The porosity at the time of deposition usually diminishes with burial because the pores are filled either by mechanical compaction, chemical compaction or cementation. In porous sandstones, pressure solution at grain contacts during tectonic compression will be an active process, leading to cleavage development. In well-lithified sandstones, however, dissolution at grain contacts will be very slight because of the stable framework caused by a high degree of cementation. This explains the absence of cleavage in well-lithified sandstones.

Figure 17 illustrates what happens to apparent long axes of initially elliptical (a) and spherical (b) quartz grains affected by increasing dissolution during tectonism. This model assumes coaxial deformation in which the cleavage develops perpendicular to the *Z*-direction of total strain and in which there is no simultaneous deposition of silica perpendicular to the *Z*-direction (*X*, *Y* and *Z* are the principal axes of the strain ellipsoid, with $X \geq Y \geq Z$). At increasing dissolution there is an apparent rotation of long axes from the bedding plane to the plane perpendicular to the *Z*-direction. The higher the dissolution, the closer the grain long axes will be oriented to the pressure-solution surfaces (*XY*-plane).

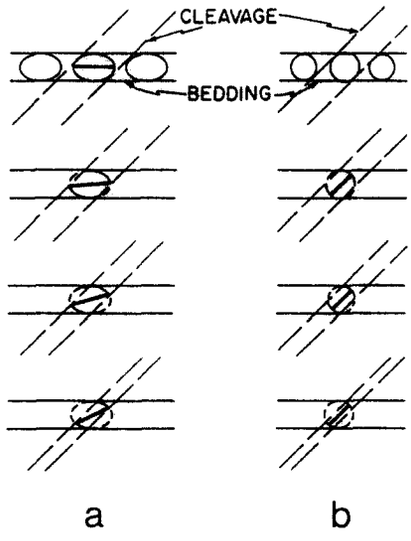

Fig. 17. A model for the development of cleavage in sandstone by pressure solution during coaxial shortening (pure shear). (a) For initially elliptical grains oriented parallel to bedding. The long axes of quartz grains (heavy black lines) rotate from subparallel to the bedding towards the pressure-solution surface. (b) For initially spherical grains. The long axis has a constant orientation.

Grain shape and grain contact orientation diagrams (Figs. 15 and 16) show that pressure solution during tectonism was not strong enough to reorient the long axes of elongated bedding-parallel grains. It was, however, sufficient to obliterate maxima parallel to bedding. Cleavage seams are only partially developed because of the low degree of dissolution and are comparable (but on a much smaller scale) to Gray's (1978, fig. 4) short and discontinuous, rough cleavage seams in wackestone. The cleavage seams are very thin and up to five quartz grains long (Fig. 12).

Pressure-solution cleavage in the studied sandstone samples is probably parallel to some average principal plane of strain (e.g. Williams 1976). It has a penetrative appearance in exposures. During folding, the bedding rotates with respect to the bulk shortening direction in the rock, and consequently the cleavage orientation is the result of strain increments applied at different orientations.

DISCUSSION

Compressional folding and associated extrusion of evaporite diapirs is favoured by most previous workers (Hoen 1964, Thorsteinsson 1974, Balkwill 1978). Such a model implies that tectonic squeezing of ductile anhydrite along hinge-faults of anticlines and thrust faults during the Tertiary Eurekan Orogeny caused all the anhydrite diapirs on Axel Heiberg Island. However, paleomagnetic data of diabase sills from the North Mokka anticline (Jackson & Halls 1985) strongly suggest that the sills were intruded during the early Cretaceous while the anticlines had grown about half way to the present amplitude. This is well before the compressional phase of the Tertiary Eurekan Orogeny. Also, there is clear stratigraphic evidence that the large evaporite diapirs influenced the sedimentation pattern already during the Upper Triassic (A. Embry personal communication 1983).

Strain patterns in overburdens of experimental diapiric ridges (e.g. Dixon 1975, van Berkel 1988) clearly show subhorizontal or gently-plunging extension axes and a normal (hangingwall block down) sense of shear. However, steep or subvertical plunging extension axes and reverse (hangingwall block up) sense of shear are characteristic of interdiapiric synforms (Dixon & Summers 1983, van Berkel 1988). The sense of bedding-parallel shear and the cleavage pattern in sandstone of the anticlines studied (Fig. 14a) are compatible with the strain pattern in the overburden of these experimental models. The cleavage pattern in flexural-slip or flexural-flow folds formed by lateral compression (Fig. 14b) is drastically different. Tangential longitudinal strain (Ramsay & Huber 1987, p. 457) forms an arcuate hinge cleavage (Roberts & Strömgard 1972, Ramsay & Huber 1987, fig. 20.50) in the *incompetent* rocks above a competent layer. However, in the North Mokka and Whitsunday Bay anticlines gently-dipping cleavages are developed in *competent* sandstone beds. Moreover, the coalescent domal structure within both anticlines can probably be formed only by diapirism (cf. Trusheim 1960).

The evaporite diapirs are cored by salt (Schwerdtner & Osadetz, 1983, Schwerdtner & van Kranendonk 1984). During the early stage of diapirism anhydrite behaved as a very plastic material because of the relatively high temperature at depth, and together with the underlying salt pierced the overburden. At shallow crustal levels anhydrite turned brittle but was so strong that salt couldn't pierce the anhydrite hood and the rigid and heavy anhydrite hoods were pushed up by the salt.

Continuing growth of the diapiric anticlines and evaporite diapirs after the Tertiary Eurekan Orogeny, if it had occurred, would have overprinted slickensides and could have formed a steep cleavage characteristic of compressional folding. It is highly unlikely that this has happened in the North Mokka and Whitsunday Bay anticlines because the internal structures of the Three Lakes diapir (Fig. 3) and the Fulmar Channel diapir (Fig. 5) are truncated at high to moderate angles by faults of the Eurekan Orogeny.

CONCLUSIONS

(1) The North Mokka and Whitsunday Bay anticlines were mainly generated by diapirism in the Mesozoic during static or extensional geologic conditions, with ductile behaviour and buoyancy of the evaporites as the main cause.

(2) The coalescent domal outline of both anticlines is probably diagnostic of diapirism.

(3) The cleavage pattern in the North Mokka and Whitsunday Bay anticlines and adjacent synclines is compatible with the strain distribution in experimental models of low-amplitude diapiric ridges if the cleavage is parallel to the XY-plane of total strain.

(4) Bedding-parallel shear, as revealed by the facing direction of fracture steps of bedding-surface slickensides, and cleavage patterns in sandstone can be used to discriminate between low-amplitude ridges formed by diapirism and folds formed by lateral compression. This cannot be done near small, high-amplitude, second-order diapirs that pierce their overburden.

(5) Pressure-solution cleavage in poorly consolidated sandstones is defined by a quartz grain shape fabric and most probably formed by quasi-homogeneous pressure solution. Cleavage seams are discontinuous and anastomosing, and their spacing is small.

Acknowledgements—Research for this paper was carried out at the University of Toronto while the author was holding a Research Associateship to W. M. Schwerdtner. I would like to thank W. M. Schwerdtner and P.-Y. F. Robin for their help and guidance. Fruitful discussions with J. Morgan, J. Torrance, P. F. Williams, H. Hugon and A. D. Miall are gratefully acknowledged. Critical reviews by P. J. Hudleston, W. M. Schwerdtner, H. E. Rondeel and two anonymous reviewers greatly improved the manuscript. The following undergraduate students acted as field assistants: L. Evans and G. Boisvert in 1982, M. J. van Kranendonk and S. Foley in 1983, and B. Wiseman in 1984.

Financial support was received from two NSERC grants, three

Northern Training Grants (Department of Indian and Northern Affairs), a research grant from the University of Toronto to W. M. Schwerdtner, and a NSERC Strategic Grant to A. D. Miall and colleagues. Logistic support was provided by Polar Continental Shelf Project (Department of Energy, Mines and Resources, Ottawa), and the Institute of Sedimentary and Petroleum Geology of the Geological Survey of Canada (Calgary).

REFERENCES

Balkwill, H. R. 1978. Evolution of Sverdrup Basin, Arctic Canada. *Bull. Am. Ass. Petrol. Geol.* **62**, 1004–1028.

Berkel, J. T. van 1985. Pressure-solution cleavage in poorly-consolidated Mesozoic sandstone of the Central Eureka Sound Fold Belt, Canadian Arctic Archipelago. In: *Proceedings of the International Conference on Tectonic and Structural Processes*. Utrecht, The Netherlands, 10–12 April 1985, 55.

Berkel, J. T. van 1986. A structural study of evaporite diapirs, folds and faults, Axel Heiberg Island, Canadian Arctic Islands. GUA Papers of Geology, Series 1, No. 26. University of Amsterdam.

Berkel, J. T. van 1988. Kinematic evaluation of a finite-element model of a diapiric ridge. *Bull. geol. Instn Univ. Uppsala* **14**, 111–114.

Berkel, J. T. van, Hugon, H., Schwerdtner, W. M. & Bouchez, J. L. 1983. Study of anticlines, faults and diapirs in the central Eureka Sound Fold Belt, Canadian Arctic Islands: preliminary results. *Bull. Can. Petrol. Geol.* **31**, 109–116.

Berkel, J. T. van, Schwerdtner, W. M. & Torrance, J. G. 1984. Origin of wall-and-basin structure—an intriguing tectonic–halokinetic feature on west-central Axel Heiberg Island, Sverdrup Basin, Canadian Arctic Archipelago. *Bull. Can. Petrol. Geol.* **32**, 343–358.

Berkel, J. T. van, Torrance, J. T. and Schwerdtner, W. M. 1986. Deformed anhydrite nodules—a new type of strain gauge in sedimentary rocks. *Tectonophysics* **124**, 309–323.

Borradaile, G. J., Bayly, M. B. & Powell, C. McA. 1982. *Atlas of Deformational and Metamorphic Rocks Fabrics*. Springer-Verlag, New York.

Dixon, J. M. 1974. A new method for determination of finite strain in models of geological structures. *Tectonophysics* **24**, 99–114.

Dixon, J. M. 1975. Finite strain and progressive deformation in models of diapiric structures. *Tectonophysics* **28**, 89–124.

Dixon, J. M. & Summers, J. M. 1983. Patterns of total and incremental strain in subsiding troughs: experimental centrifuged models of inter-diapiric synclines. *Can. J. Earth Sci.* **20**, 1843–1861.

Durney, D. W. 1972. Solution transfer, an important geological deformation mechanism. *Nature* **235**, 315–317.

Embry, A. F. 1982. The Upper Triassic–Lower Jurassic Heiberg deltaic complex of the Sverdrup Basin. In: *Arctic Geology and Geophysics* (edited by Embry A. F. & Balkwill, H. R.). *Mem. Can. Soc. Petrol. Geol.* **8**, 189–217.

Fletcher, R. C. 1972. Application of a mathematical model to the emplacement of mantled gneiss domes. *Am. J. Sci.* **272**, 197–216.

Gould, D. B. & DeMille, C. 1964. Piercement structures in the Arctic Islands. *Bull. Can Petrol. Geol.* **12**, 719–753.

Gray, D. R. 1978. Cleavage in deformed psammitic rocks from southeastern Australia: their nature and origin. *Bull. geol. Soc. Am.* **89**, 577–590.

Hancock, P. L. & Barka, A. A. Kinematic indicators on active normal faults in western Turkey. *J. Struct. Geol.* **9**, 573–584.

Heald, M. T. 1956. Cementation of Simpson and St. Peter sandstones in parts of Oklahoma, Arkansas and Missouri. *J. Geol.* **64**, 16–30.

Hoen, E. W. 1964. The anhydrite diapirs of central–western Axel Heiberg Island. Axel Heiberg Island Research Reports, Geology, No. 2, McGill University, Montreal.

Hoeppener, R. 1955. Tectonik im Schiefergebirge. *Geol. Rdsch.* **44**, 26–55.

Hugon, H. & Schwerdtner, W. M. 1982. Discovery of large amounts of halite in a small evaporite diapir on south-eastern Axel Heiberg Island, Canadian Arctic Archipelago. *Bull. Can. Petrol. Geol.* **30**, 303–305.

Jackson, K. C. & Halls, H. C. 1985. A test for the timing of folding of the North Mokka Anticline using paleomagnetic data from diabase sills, eastern Axel Heiberg Island, Canadian Arctic Archipelago. *Bull. Can. Petrol. Geol.* **33**, 227–235.

Mareschal, J.-C. & West, G. F. 1977. Two-dimensional finite element modelling of geological deformation by thermally stimulated creeping flow. Annual report Negotiated Development Grant to study the continental crust and its mineral deposits. University of Toronto, 1 December 1977.

Mareschal, J.-C. & West, G. F. 1980. A model for Archean tectonism. Part 2. Numerical models of vertical tectonism in greenstone belts. *Can. J. Earth Sci.* **17**, 60–71.

Morgan, J. 1986. Three-dimensional strain in centrifuge models and an Archean greenstone belt. Unpublished Ph.D. Thesis, University of Toronto.

Nassichuk, W. W. & Davies, G. R. 1980. Stratigraphy and sedimentation of the Otto Fiord Formation. *Bull. geol. Surv. Can.* **286**.

Norris, D. K. & Barron, K. 1969. Structural analysis of features on natural and artificial faults. In: *Proceedings of the Conference on Research in Tectonics–Kink Bands and Brittle Deformation*, Ottawa, March 1968 (edited by Baer, A. J. & Norris, D. K.). *Geol. Surv. Pap. Can.* **68-52**, 136–172.

Petit, J. P. 1987. Criteria for the sense of movement on fault surfaces in brittle rocks. *J. Struct. Geol.* **9**, 597–608.

Pettijohn, F. J., Potter, P. E. & Siever, R. 1973. *Sand and Sandstone*. Springer-Verlag, New York.

Plessman, W. 1963. Lösung, Verformung, Transport, und Gefüge (Beitrage zür Gesteinsverformung in nordöstlichen Rheinisch Schiefergebirge). *Z. dt. geol. Ges.* **115**, 650–663.

Ramberg, H. 1963. Strain distribution and geometry of folds. *Bull. geol. Instn Univ. Uppsala* **42**, 1–20.

Ramberg, H. 1967. *Gravity, Deformation and the Earth's Crust*. Academic Press, London.

Ramberg, H. 1981. *Gravity, Deformation and the Earth's Crust* (2nd edn). Academic Press, London.

Ramsay, J. G. 1967. *Folding and Fracturing of Rocks*. McGraw-Hill, New York.

Ramsay, J. G. & Huber, M. I. 1987. *The Techniques of Modern Structural Geology. Volume 2: Folds and Faults*. Academic Press, New York.

Roberts, D. & Strömgard, K. E. 1972. A comparison of natural and experimental strain patterns around fold hinge zones. *Tectonophysics* **14**, 105–120.

Schwerdtner, W. M. & Clark, A. R. 1967. Structural analysis of Mokka Fiord and South Fiord Domes, Axel Heiberg Island, Canadian Arctic. *Can. J. Earth Sci.* **4**, 1229–1245.

Schwerdtner, W. M. & Osadetz, K. 1983. Evaporite diapirism in the Sverdrup Basin: new insights and unsolved problems. *Bull. Can. Petrol. Geol.* **32**, 27–36.

Schwerdtner, W. M. & Tröeng, B. 1978. Strain distribution within arcuate diapiric ridges of silicone putty. *Tectonophysics* **50**, 13–28.

Schwerdtner, W. M. & van Kranendonk, M. J. 1984. Structure of Stolz Diapir—a well-exposed salt dome on Axel Heiberg Island. *Bull. Can. Petrol. Geol.* **32**, 237–241.

Schwerdtner, W. M., Sutcliffe, R. H. & Tröeng, B. 1978. Patterns of total strain in the crestal region of immature diapirs. *Can. J. Earth Sci.* **15**, 1437–1447.

Sibley, D. F. & Blatt, H. 1976. Intergranular pressure solution and cementation in the Tuscarora orthoquartzite. *J. sedim. Petrol.* **46**, 881–896.

Stephansson, O. 1972. Theoretical and experimental studies of diapiric structures on Öland. *Bull. geol. Instn. Univ. Uppsala* **3**, 163–200.

Talbot, C. J. 1977. Inclined and asymmetric upward-moving gravity structures. *Tectonophysics* **42**, 159–181.

Thorsteinsson, R. 1974. Carboniferous and Permian stratigraphy on Axel Heiberg Island and western Ellesmere Island, Canadian Arctic Archipelago. *Bull. geol. Surv. Can.* **224**.

Thorsteinsson, R. & Tozer, E. T. 1970. Geology of the Arctic Archipelago. In: *Geology and Economic Minerals of Canada* (edited by Douglas, R. J. W.). *Geol. Surv. Can., Econ. Report* **1**, 548–590.

Tjia, H. D. 1964. Slickensides and fault movements. *Bull. geol. Soc. Am.* **75**, 683–686.

Tjia, H. D. 1967. Sense of fault displacements. *Geologie Mijnb.* **46**, 392–396.

Trusheim, F. 1960. Mechanism of salt migration in northern Germany. *Bull. Am. Ass. Petrol.* **44**, 1519–1540.

West, G. F. & Mareschal, J.-C. 1979. A model for Archean tectonism. Part 1. The thermal conditions. *Can. J. Earth Sci.* **16**, 1942–1950.

Williams, P. F. 1972. Development of metamorphic layering and cleavage in low grade metamorphic rocks at Bermagui, Australia. *Am. J. Sci.* **272**, 1–47.

Williams, P. F. 1976. Relationships between axial-plane foliations and strain. *Tectonophysics* **30**, 181–196.